

Influence of the heat transfer model on the estimation of mass transfer

Maria Giovanna Rodio, Pietro Marco Congedo

► **To cite this version:**

| Maria Giovanna Rodio, Pietro Marco Congedo. Influence of the heat transfer model on the estimation of mass transfer. [Research Report] RR-8438, INRIA. 2013. <hal-00922784>

HAL Id: hal-00922784

<https://hal.inria.fr/hal-00922784>

Submitted on 30 Dec 2013

HAL is a multi-disciplinary open access archive for the deposit and dissemination of scientific research documents, whether they are published or not. The documents may come from teaching and research institutions in France or abroad, or from public or private research centers.

L'archive ouverte pluridisciplinaire **HAL**, est destinée au dépôt et à la diffusion de documents scientifiques de niveau recherche, publiés ou non, émanant des établissements d'enseignement et de recherche français ou étrangers, des laboratoires publics ou privés.



Influence of the heat transfer model on the estimation of mass transfer.

Maria Giovanna Rodio, Pietro Marco Congedo

**RESEARCH
REPORT**

N° 8438

December 2013

Project-Teams Bacchus



Influence of the heat transfer model on the estimation of mass transfer.

Maria Giovanna Rodio, Pietro Marco Congedo

Project-Teams Bacchus

Research Report n° 8438 — December 2013 — 10 pages

Abstract: The efficient design and performance of turbopumps in rocket propulsion systems demands a robust numerical tool predicting the phenomenon of cavitation in cryogenic fluids. Building robust models for this complex physics, according to a not-large set of experimental data, is very challenging. In fact, cryogenic fluids are thermo-sensitive, and therefore, thermal effects and strong variations in fluid properties can alter the cavitation properties. This work illustrates how thermal effects can be estimated considering both convective and conductive heat transfer. The Rayleigh-Plesset (RP) equation is coupled with a bubbly flow model to assess the prediction of thermal effects, and used in order to simulate some reference experimental test-cases in literature. Moreover, some tuning parameters, not measured experimentally, such as initial volume vapor phase α_0 and initial radius bubbles R_0 and the specific coefficient of the heat transfer models are treated like epistemic uncertainties in a probabilistic framework, permitting to obtain numerical error bars for some quantities of interest, and then to perform a robust analysis of the thermal effect.

Key-words: Cavitation, cryogenic fluids, convection and conduction, thermal effect.

**RESEARCH CENTRE
BORDEAUX – SUD-OUEST**

351, Cours de la Libération
Bâtiment A 29
33405 Talence Cedex

Etude de l'influence du modèle de transfert de chaleur sur l'estimation de l'échange de masse

Résumé : La précision des simulations numériques pour la prédiction du phénomène de cavitation (formation des bulles de gaz dans le liquide) est très importante pour l'optimisation des performances des moteurs aérospatiaux. Le carburant utilisé pour la propulsion de ces moteurs sont des mélanges de fluides cryogéniques dans lesquelles le phénomène de cavitation se développe souvent. Les fluides Cryogéniques sont des fluides thermo-sensible, et par conséquent, les effets thermiques et les variations de leur propriétés physique peuvent modifier le développement de la cavitation. Le but de ce travail est d'analyser comment l'échange thermique, entre le liquide et les bulles générées par la cavitation, est influencé par des paramètres qui sont présents dans le modèle physique, pour améliorer la prédiction des effets thermiques et, donc, de la cavitation.

L'équation de Rayleigh-Plesset, qui permet d'estimer le rayon de la bulle, est couplée avec un modèle 'Bubbly flow' pour prendre en compte l'effet thermique. Les paramètres du modèle appelés de 'tuning', qui ne sont pas mesurés expérimentalement, comment la fraction volumique initiale de vapeur α_0 , le rayon initial de la bulle R_0 et le coefficient h_b ou ϵ du modèle de transfert thermique sont considérés comme des incertitudes de type épistémique. Cette étude permet d'obtenir les bars d'erreur numérique pour les quantités d'intérêt et d'obtenir une analyse robuste de l'effet thermique. De différents cas test expérimentaux connus en littérature ont été simulés .

Mots-clés : Cavitation, fluides cryogéniques, transfert par convection, transfert par conduction, effet thermique

Contents

1	Introduction	3
2	Governing equations	4
3	Thermodynamic Effects	4
3.0.1	<i>Convective Approach</i>	5
3.0.2	<i>Conductive Approach</i>	5
3.0.3	<i>Complete Model and Numerical Method</i>	5
3.1	Stochastic Method	6
4	Results	6
4.1	Conductive effects and comparison with convective ones	7
4.2	Stochastic computations considering uncertainties	7
5	Conclusions	8

1 Introduction

One of the major source of degradation of the performance and useful life of turbopumps, and of the dramatic increase of the noise generation is represented by the cavitation. It is a phenomenon characterized by the formation of vapor bubbles in the liquid, due to a local reduction of pressure below vapor pressure, corresponding to liquid temperature. For this reason, the cavitation is usually considered as an isothermal phenomenon, but this hypothesis is no longer valid in the case of cryogenic fluids, used as turbopumps propellant. These fluids are particularly prone to cavitation, because they are used in critical conditions. Moreover, during the transition phase, a drop in the liquid temperature has been observed experimentally. This temperature reduction is the consequence of the bubble heat absorption from the liquid phase during the cavitation mechanism. The temperature drop is called "thermal effect" (see [1, 2] for more details). Then, the temperature difference produces a different vapor pressure and a variation in the fluid properties, such as the growth or collapse of the bubble. So, including the effect of heat transfer in the cavitation model is necessary for the correct prediction of cavitation behaviour. The thermal effect is based on a thermal non-equilibrium state, where the phase temperatures are different at the interface between the phases (i.e. there is a discontinuity at the interface). So heat transfer develops following both thermal conduction and convection. In literature, few studies [3] had been devoted to the analysis of both the heat exchange mechanism, *i.e.* convective and conductive, for the estimation of thermal effect in cryogenic cavitating flows. When considering heat exchange between the two phases, a convective heat coefficient, h_b , or a heat transfer enhancement coefficient, ε , in a conductive approach, are introduced. Each of these parameters appear in the RP equation. In this work, we consider h_b and ε as a constant obtained by means of some empirical assumptions as shown [3, 4]. Seeing that very few experimental data exist concerning the value of these parameters for cryogenic flows, a sensitivity analysis of optimal range value of both parameters is necessary. Previously, in [2], the authors proposed

a sensitivity analysis of the convective heat transfer coefficient, h_b , in hydrodynamic and cryogenic cavitation at high Reynolds numbers. They verified that the different values of h_b correspond to different cavitating regimes determined by a bubbles growth based on mechanical forces or *thermal effect* force.

The originality of this paper is twofold. First, the analysis already developed in [2] is extended considering both h_b coefficient and ε coefficient. The aim is to obtain an optimized value of h_b and of ε for cryogenic cavitation (the working fluid is hydrogen). Secondly, an uncertainty quantification is performed for taking into account the unknown parameters of the model that are not measured experimentally, but that represent the tuning parameters of the model. The uncertainties parameters chosen in this study are the initial volume vapor fraction α_0 , the initial bubble radius R_0 and the h_b or the ε coefficient for the convective and the conductive model, respectively. All the uncertainties are treated like epistemic uncertainties using a Polynomial Chaos technique [5].

2 Governing equations

The proposed model is able to reproduce a quasi-one-dimensional steady flow in a converging-diverging nozzle. The continuity and momentum equations are solved for the bubbly flow coupled with a equation to define the volume fraction and the Rayleigh-Plesset equation for the evolution of bubble radius. A convective and a conductive heat transfer models are coupled to this cavitation model. At the initial or upstream condition, the liquid and the bubbles are in dynamic and thermal equilibrium. At any given nozzle cross-section, the bubbles have a uniform size and their number is constant in the duct. Therefore, the bubbles are composed of vapor and gas, and the temperature and pressure within them are always uniform. The bubble and the liquid temperature are equal at the interface, there is no friction or heat transfer between the flow and the nozzle walls and the liquid and vapor densities, ρ_l and ρ_v , are constant.

3 Thermodynamic Effects

Assuming that the bubble is perfectly spherical, bubble growth can be modeled using the well-known Rayleigh-Plesset equation (RP):

$$R \frac{D^2 R}{Dt^2} + \frac{3}{2} \left(\frac{DR}{Dt} \right)^2 + \underbrace{\frac{4\nu_l DR}{R Dt}}_{\text{viscosity term}} + \underbrace{\frac{2S}{\rho_l R}}_{\text{surface tension term}} = \underbrace{\frac{p_{g0}}{\rho_l} \left(\frac{R_0}{R} \right)^{3\gamma}}_{\text{incondensable gas term}} + \underbrace{\frac{P_v(T_\infty) - p(x, t)}{\rho_l}}_{\text{mechanical term}} + \underbrace{\frac{P_v(T_b(x, t)) - P_v(T_\infty)}{\rho_l}}_{\text{thermal effect term}}, \quad (1)$$

where D/Dt is a Lagrangian derivative, ν_l is the liquid viscosity, S is the superficial tension, ρ_l is the liquid density, $T_b(x, t)$ is the bubble temperature and T_∞ is the flow temperature located away from the bubbles and corresponding to the upstream liquid temperature, p_{g0} is the incondensable gas pressure and $\gamma = 1.4$ is the coefficient of the polytropic law. As explained by Brennen [1]

(see also by Franc [3]), the last term of Eq.(1) can be transformed by a Taylor expansion in a temperature difference as follows:

$$P_v(T_b(x, t)) - P_v(T_\infty) = (dP_v/dT)(T_b(x, t) - T_\infty).$$

In the case of the isothermal hypothesis, $T_b(x, t) = T_\infty$, otherwise, this difference can be estimated by a convective or a conductive heat transfer model.

3.0.1 Convective Approach

In the case of convective heat transfer the temperature difference is calculated by balancing the latent heat associated with evaporation or (condensation) with the heat exchanged between the liquid and the bubble:

$$\frac{D}{Dt} \left(\frac{4}{3} \pi R^3 \rho_v \right) L_{ev} = 4\pi R^2 h_b (T_\infty - T_b(x, t)), \quad (2)$$

where ρ_v is the vapor density and L_{ev} is the liquid latent heat. h_b is the bubble convective heat transfer coefficient and it represents the uncertainty parameter of the this approach.

3.0.2 Conductive Approach

Supposing a conductive heat transfer, Plesset and Zwick proposed an explicit expression of the bubble wall temperature [6]. The difference of temperature is estimated as follows:

$$B = \frac{T_\infty - T_b}{\Delta T^*} = \frac{1}{\sqrt{\pi \varepsilon \lambda_l}} \int_{u=0}^{u=t} \frac{R^2(u) \frac{dR(u)}{dt} du}{\sqrt{\int_{v=u}^{v=t} R^4(v) dv}} \quad (3)$$

where λ_l is the liquid diffusivity. ε is the heat transfer enhancement coefficient defined as the ratio between the the turbulent and the liquid diffusivity λ_t/λ_l or between the turbulent and the liquid thermal conductivity δ_t/δ_l . It was shown, in previous studies [3], that, for example, in the case of R114 fluid, this coefficient can vary in a very large range of values. For other fluids, as in the case of hydrogen fluid, this coefficient is not known and, thus, it has been treated as an uncertainty in the conductive approach.

3.0.3 Complete Model and Numerical Method

The complete steady 1D model considered in this work assumes the following form:

$$\left\{ \begin{array}{l} (1 - \alpha) \bar{u} \bar{A} = (1 - \alpha_0) = \text{constant} \\ \bar{u} \frac{d\bar{u}}{d\bar{x}} = -\frac{1}{2(1 - \alpha)} \frac{dCp}{d\bar{x}} \\ \bar{R} \left(\bar{u}^2 \frac{d^2 \bar{R}}{d\bar{x}^2} + \bar{u} \frac{d\bar{u}}{d\bar{x}} \frac{d\bar{R}}{d\bar{x}} \right) + \frac{3\bar{u}^2}{2} \left(\frac{d\bar{R}}{d\bar{x}} \right)^2 + \frac{4\bar{u}}{Re\bar{R}} \frac{d\bar{R}}{d\bar{x}} + \frac{2}{We} \left(\frac{1}{\bar{R}} - \frac{1}{\bar{R}^{3\gamma}} \right) = \\ \quad -\frac{Cp}{2} - \frac{\sigma}{2} \left(1 - \frac{1}{\bar{R}^{3\gamma}} \right) + \text{Heat transfer term} \end{array} \right.$$

RR n° 8438

$$\left\{ \begin{array}{l} \text{Heat transfer term} = \left\{ \begin{array}{l} -\frac{dP_v}{dT} \frac{L_{ev} \rho_v}{\rho_l h_b u_0} \bar{u} \frac{d\bar{R}}{d\bar{x}} \\ -\frac{dP_v}{dT} \frac{\Delta T^*}{\rho_l u_0^2 \bar{u}^2 \bar{R}} \sqrt{\frac{R_0 u_0}{\pi \varepsilon \lambda_l}} \int_{u=0}^{u=x} \frac{\bar{R}^2(u) \frac{d\bar{R}(u)}{d\bar{x}} du}{\sqrt{\int_{v=u}^{v=x} \frac{\bar{R}^4}{\bar{u}}(v) dv}} \end{array} \right. \begin{array}{l} \text{Convective Approach} \\ \text{Conductive Approach} \end{array} \end{array} \right.$$

As it can be seen, this is a dimensionless system, where the reference values are assumed as follows: $\bar{u} = u/u_0$, $\bar{x} = x/R_0$, $\bar{R} = R/R_0$, $\bar{\eta} = \eta R_0$, $\bar{L} = L/R_0$, $\bar{t} = tu_0/R_0$. Note that the upstream conditions are denoted by the subscript "0", while the dimensionless variables are denoted by superscript "-", and t is the time, u is the velocity of flow, R is the bubble radius, η is the bubble population for a unit of liquid volume (obtained by considering the relation $(1 - \alpha_0) = 1/(1 + 4/3\pi\bar{\eta})$), and L is the length of the nozzle. The upstream gas pressure is obtained by applying the Laplace law at the upstream condition, $p_{g0} = p_0 + 2S/R_0$, where S is the surface tension. These relations allow the introduction of the dimensionless Reynolds number $Re = \rho_l u_0 R_0 / \mu$, the dimensionless Weber number, $We = \rho_l u_0^2 R_0 / S$ and the cavitation number $\sigma = (p_0 - P_v(T_\infty)) / (0.5 \rho_l u_0^2)$ into the equations.

3.1 Stochastic Method

In this paper, the non-intrusive spectral projection method is used for taking into account the uncertainties (see [5, 7]), a random variable ξ (whose dimension depends on the number of uncertain parameters in the problem). Under specific conditions, a stochastic process can be expressed as a spectral expansion based on suitable orthogonal polynomials, with weights associated with a orthogonal polynomials, with weights associated with a particular probability density function. The first study in this field is the Wiener (1938) process. The basic idea is to project the variables of the problem onto a stochastic space spanned by a complete set of orthogonal polynomials Ψ that are functions of random variables ξ . For example, the unknown variable ϕ has the following spectral representation:

$$\phi(\mathbf{x}, \theta) = \sum_{i=0}^{\infty} \phi_i(\mathbf{x}) \Psi_i(\xi(\theta)) \quad (4)$$

Substituting the polynomial chaos expansion (4) into our stochastic problem, and applying a collocation projection, the coefficients $\phi_i(\mathbf{x})$ are obtained using quadrature formulae based on tensor product of a 1D formula. Then, a deterministic problem for each collocation point is performed. In both cases, once the chaos polynomials and the associated ϕ_i coefficients have been determined, the expected value and the variance of the stochastic solution $\phi_i(\mathbf{x}, \theta)$ are computed from $E_{PC} = \phi_0(\mathbf{x})$, and $Var_{PC} = \sum_{i=0}^N \phi_i^2(\mathbf{x}) \langle \Psi^2 \rangle$, respectively. Another interesting property of PC expansion is to make easier sensitivity analysis based on the analysis of variance decomposition (ANOVA). ANOVA allows identifying the contribution of a given stochastic parameter to the total variance of an output quantity. For further details, see Congedo *et al.*[5]. This method allows reducing the stochastic problem into a series of deterministic runs where specific values for parameters affected by uncertainties are considered. Then, the CFD solver is not modified and it remains completely decoupled from the stochastic code.

4 Results

In this study, the cavitating test case 134 [8] (see table 1) in a Venturi orifice has been reproduced. The numerical domain and its dimensionless area are shown

in figure (1).

Test Case	Cavity Length [cm]	T_0 [K]	V_0 [m/s]	P_0 [N/cm ²]	σ
134	5.08	20.69	58.7	36.02	2.01

Table 1: Operating conditions of Hord test case 134 [8].

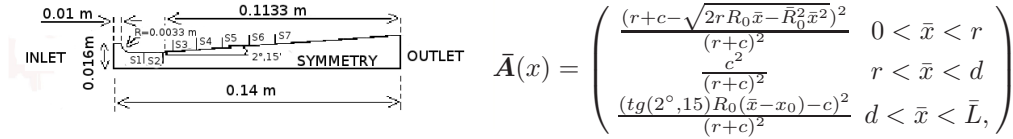


Figure 1: Schematic view of Venturi profile. S1-S7 represent sensor positions. \bar{A} is the dimensionless area, where $r = 0.0033m$, $c = 0.01238250m$, $d = 0.016764m$ and $x_0 = 0.016764m$

4.1 Conductive effects and comparison with convective ones

In order to make a consistent comparison between conductive and convective approaches, an optimization study on the tuning parameters is performed. Hence, a genetic algorithm based method [5] is used to optimize h_b (varying in $1 \times 10^3 \div 1 \times 10^{10}$ W/(m²K) and ε (varying in $1 \div 1 \times 10^{-10}$) for the convective and the conductive approach, respectively, and α_0 ($1 \times 10^{-10} \div 1 \times 10^{-03}$) and R_0 ($5 \times 10^{-4} \div 5 \times 10^{-5}$). A bi-objectives optimization is performed to calibrate the numerical solution to the experiments in terms of pressure and temperature. Values of optimized parameters are summarized in table 2. Temperature and pressure estimation along the Venturi show a very good agreement with the experimental results near the throat, corresponding to $x < 0.02$ (see figures (2) (a-b)). Differences increase for greater values of x . Error on the temperature is larger than for the pressure, obtaining a maximum error at $x = 0.078m$ equal to nearly 15% and to 19% for the temperature and the pressure, respectively. A numerical cavitation length of nearly 5 cm, as in the experimental observation, is obtained imposing an α value of 0.045 and of 0.05 for the conductive and the convective approaches, respectively (see figure (2) (c)).

	α_0	R_0 [m]	h_b	ε
Convective	1.1×10^{-3}	1×10^{-4}	3.0×10^{-3}	-
Conductive	1.6×10^{-3}	1×10^{-4}	-	$1 \times 10^{-6.3}$

Table 2: Optimized parameters for convective and conductive approaches.

4.2 Stochastic computations considering uncertainties

After optimizing the tuning coefficients for convection and conduction, a sensitivity study is performed, considering three uncertainties for each approach: h_b for the convective or ε for the conductive, with α_0 and R_0 for both. A variation of 1% is imposed. Seeing that an accurate estimation of probability density function for these epistemic parameters is not possible, a uniform pdf is used. This choice represents a robust safety strategy in order to check uncertainty

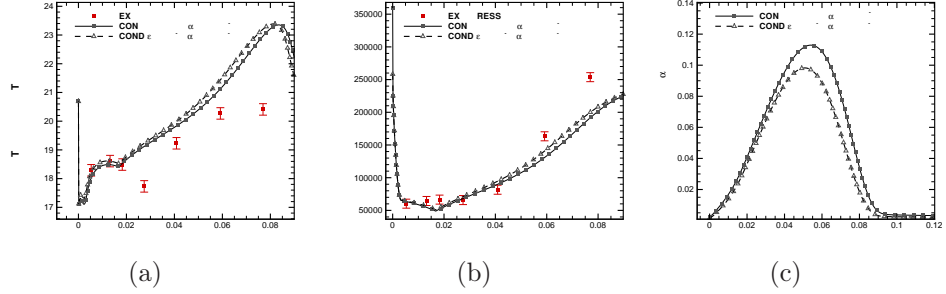


Figure 2: Comparison of numerical solutions and experiments in terms T_b (a), liquid pressure P_l (b), and α obtained with both convective and conductive approaches.

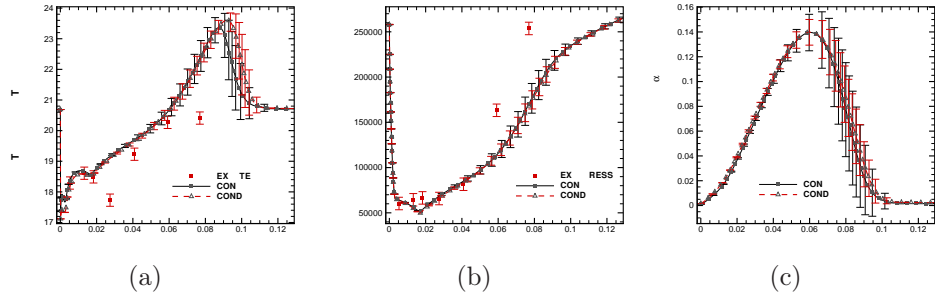


Figure 3: Stochastic evolution of bubble temperature T_b , liquid pressure P_l and vapor fraction, obtained with convective and conductive approaches, when considering uncertainties.

propagation of physical uncertainties. In figure 3, numerical error bars associated to the pressure are very tiny, then pressure is not very sensitive to the considered uncertainties. Concerning temperature and vapor fraction, solutions are not sensitive for $x < 0.06$, while larger numerical error bars are observed for an increasing x . Coefficient of variation (mean to standard deviation ratio) is greater than 5% for some points. This means that the temperature and vapor fraction are not well predicted when considering uncertainties. Finally, in figure 4, the contribution of each uncertainty on the global variance of T_b is reported for both convective and conduction approaches (note that the % contribution is multiplied by the variance). Concerning the convective one, contributions of uncertainties on h_b and R_0 are very similar and predominant with respect to α_0 . A different result is observed for the conductive approach, where the contribution of the R_0 uncertainty is the most predominant.

5 Conclusions

This paper is devoted to the analysis of the heat exchange mechanisms, *i.e.* convective and conductive, between the vapor and the liquid phases during the development of cavitation phenomenon in cryogenic flows. For these fluids, as

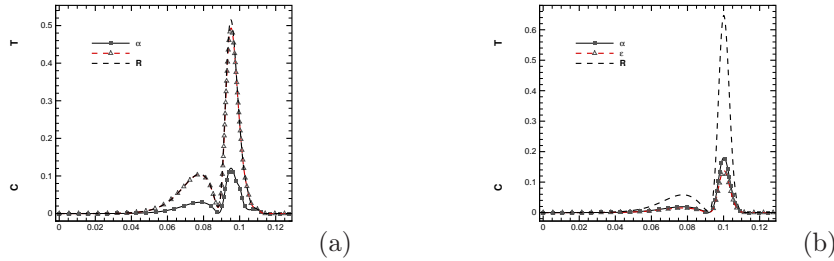


Figure 4: Contribution to the variance of T_b of each source of uncertainty for the convection (a) and conductive (b) case.

liquid hydrogen, oxygen and so on, the cavitation is characterized by a pressure drop and temperature drop, too, that can not be negligible (thermal effect) and it influences the bubbles grow.

The cavitating flow is reproduced by coupling a bubbly flow model that solves the conservative equations for the liquid phase, with the Rayleigh-Plesset (RP) equation for the bubble radius evolution and a transport equation of the vapor volume fraction. When considering heat exchange between the two phases, a convective heat coefficient, h_b , or a heat transfer enhancement coefficient, ε , in a conductive approach, are introduced in the RP equation.

Both the coefficients are constant in this work and they are considered the unknowns of system, because of very few experimental data exist concerning the value of these parameters for cryogenic flows. In addition of them, the initial vapor fraction α_0 and the initial radius R_0 are taken as unknowns of the model. At first, the analysis already developed in [2] is extended on both h_b coefficient and ε coefficient, to verify their influence on the cavitating regime development. Then, all the unknowns are considered uncertainties and they are treated like epistemic uncertainties using a Polynomial Chaos technique [5]. This analysis allows to verify the influence of uncertainties propagation in the flow properties in terms of the temperature, pressure and vapor fraction profiles.

A genetic algorithm based method [5] is used to optimize h_b and ε for the convective and the conductive approach, respectively, and α_0 and R_0 . A bi-objectives optimization is performed to calibrate the numerical solution to the experiments in terms of pressure and temperature. The two approaches are compared. Temperature and pressure estimation along the Venturi show a very good agreement with the experimental results near the throat ($x < 0.02$). Differences increase for greater values of x . Error on the temperature is larger than for the pressure, obtaining a maximum error at $x = 0.078$ m equal to nearly 15% and to 19% for the temperature and the pressure, respectively.

After optimizing the tuning coefficients for convection and conduction, a sensitivity study is performed, considering 1% of variation of uncertainties. Numerical error bars associated to the pressure are very tiny, then pressure is not very sensitive to the considered uncertainties. Concerning temperature and vapor fraction, solutions are not sensitive for $x < 0.06$, while larger numerical error bars are observed for an increasing x .

References

- [1] Brennen C 1995 *Cavitation and Bubble Dynamics* (Oxford University Press) ISBN 0-19-509409-3
- [2] MG Rodio MG De Giorgi A F 2012 *International Journal of Heat and Mass Transfer* **55** 6538–6554
- [3] Franc J and Pellone C 2007 *Journal of Fluids Engineering* **129** 974–983
- [4] Watanabe S, Furukawa A and Yoshida Y 2008 *International Journal of Rotating Machinery* **2008** 1–8
- [5] Congedo P M, Corre C and Martinez J M 2011 *Computer Methods in Applied Mechanics and Engineering* **200** 216 – 232
- [6] Plesset M and Zwick S 1952 *J. Fluids Eng.* **126** 716 – 723
- [7] Crestaux T, Le Maître O and Martinez J M 2009 *Reliability Engineering & System Safety* **94** 1161–1172
- [8] Hord J 1973 Cavitation in liquid cryogenic, i-venturi Nasa cr-2054



**RESEARCH CENTRE
BORDEAUX – SUD-OUEST**

351, Cours de la Libération
Bâtiment A 29
33405 Talence Cedex

Publisher
Inria
Domaine de Voluceau - Rocquencourt
BP 105 - 78153 Le Chesnay Cedex
inria.fr

ISSN 0249-6399